Internal Mass Flux through Frost

Satoshi Fukada
Dept. of Applied Quantum Physics and Nuclear Engineering, Graduate School of Engineering, Kyushu University, Fukuoka 812-8581, Japan

Kunihiro Inoue
Kobe Steel, Wakihama, Chuo-ku, Kobe 651-0072, Japan

An experimental method is developed for determining the internal mass flux through frost with a dendrite structure. The theory and experimental procedures of the measurements using water slightly concentrated with deuterium are described. The internal mass flux determined from variations in the deuterium concentration in frost with time shows an almost linear decrease in the frost depth direction from the surface. The profile of the local frost density is almost flat in the depth direction. The frost uniformity is kept independent of the cooled-plate temperature and the total pressure in the container unless part of the frost melts. The cause for the uniformity of frost density is discussed in terms of the frost temperature profile and microscopic crystal growth.

Introduction

A desublimation process is an effective method for separating vapor from a gas mixture. The process was applied to cryogenic freezer systems for impurity removal in the fuel cycle of a thermonuclear fusion reactor (Fukada et al., 1989a,b, 1998). Heat and mass are simultaneously transferred in freezers, and mist formation and frost formation occur there. Fukada et al. (1989a,b, 1995a,b) determined rates of vapor desublimation, mist deposition and frost growth, the total heat flux, and the effective frost thermal conductivity. These data were obtained using an apparatus comprising two horizontal plates maintained at different temperatures in a closed container and another one with a vertical circular tube maintained at a constant temperature. The frost thickness, the average frost density, and the Nu and Sh numbers were successfully correlated with several relations in a frame of our understanding of natural convection between the horizontal parallel plates or of the forced and natural convection flow in a vertical circular tube. Previously, frost properties under the forced and natural convection flow were also studied by Brian et al. (1970), Yamakawa et al. (1971), Hayashi et al. (1977b), and White and Cremers (1981). Their experimental results were in good agreement with numerical ones calculated by the overall material and heat balance equations on cooled plates.

On the other hand, the following two questions have not been resolved: (1) What is the cause for frost uniformity in the direction perpendicular to a cooled plate? (2) What is the effective frost thermal conductivity independent of the total pressure? With regard to the first question, Brian et al. (1970) determined local frost-density profiles experimentally. They observed that the frost density is uniform over frost in the perpendicular direction. If the local frost-density profile is flat, a question is raised: How has the uniformity been made up? This question comes from the fact that the vapor diffusion rate evaluated from the saturation vapor-pressure profile in frost cannot make up the uniform local density profile (Brian et al., 1970; Dietenberger, 1983). In other words, the linear internal mass flux related to the uniform frost is inconsistent with the saturation vapor-pressure profile in frost. The second question is related to the fact that the pressure dependence of the frost thermal conductivity is not consistent with effective thermal conductivity models that were independently proposed for porous materials by Woodside (1958), Biguria and Wenzel (1970), Yamakawa and Otani (1972), Jones and Parker (1975), and Hayashi et al. (1977a). Any expression of their models was derived from the following two contributions: the intrinsic thermal conduction through dendrite frost and the latent heat flux due to vapor diffusion through the frost inside. The contribution of the vapor diffusion to the thermal conductivity is considered dominant below atmospheric pressure or under the low frost density. Therefore the effective frost thermal conductivity should depend on the total pressure. This is because the diffusion coefficient of water vapor in air is reversible in proportion to the

Correspondence concerning this article should be addressed to S. Fukada.

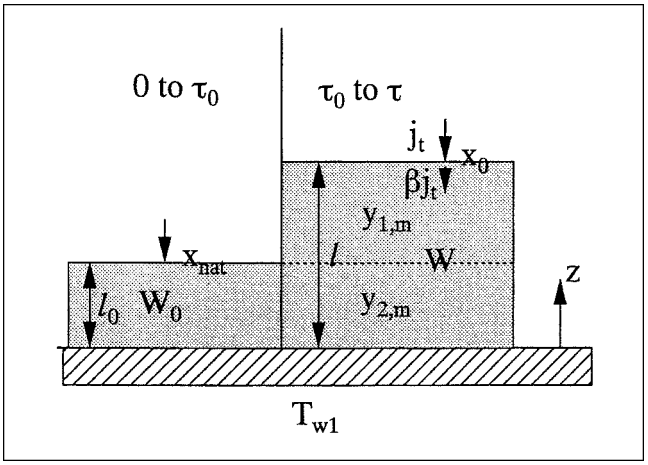

Figure 1. Procedures for determining internal mass flux inside frost by use of heavy water.

total pressure. However, our experimental result (Fukada et al., 1995b) showed that the effective frost thermal conductivity is almost independent of the total pressure.

No experimental work has been done on measuring the internal mass flux directly. This is because the internal mass flux was very difficult to determine as it is. A new method to obtain the internal mass flux was developed using water with a slight concentration of deuterium. The theory and experimental procedures of the measurement are described in the present article. The experimental internal mass flux determined from the deuterium concentration profile is compared with various hypothetical internal mass-flux profiles.

Method for Measuring Internal Mass Flux

Figure 1 explains the procedure for measuring the local frost density profile or the internal mass flux. At first, water vapor with the natural abundance of the deuterium concentration ($x_{nat} = 150$ ppm) is evaporated from a pool of heated water on the lower side of a container and is deposited on a cooled surface of the upper side. The deposition time is τ_0. The frost thickness, l_0, and the mass deposited per unit surface area, W_0, are determined at τ_0. Next, water vapor of a higher deuterium concentration is evaporated and is deposited on the frost surface from τ_0 to τ. The deuterium mole fraction on the frost surface, x_0, is kept constant from τ_0 to τ. The total mass deposition per unit surface area, W, and the frost thickness, l, are determined at τ.

Part of the heavy water vapor reaching the frost surface is spent for frost growing in the perpendicular direction, that is, an increase in frost height. The rest of it diffuses inside and is spent for making the frost dense, that is, frost growing in the horizontal direction. The perpendicular frost growth leads to a difference in the deuterium mole fraction inside the frost, y. Then the material balance of deuterium over the frost at τ is expressed in terms of W_0, W, l_0, l, x_{nat}, and x_0 as follows:

$$(W - W_0)x_0 + W_0 x_{nat} = \int_0^{l_0} \rho_z(z,\tau)\, y\, dz + \int_{l_0}^{l} \rho_z(z,\tau)\, y\, dz. \quad (1)$$

Here, $\rho_z(z,t)$ is the local frost density profile in the perpendicular direction and is a function of z and t. The local frost density is assumed uniform in the horizontal direction. When x_{nat} is much smaller than x_0, the second term on the left-hand side of Eq. 1 can be neglected. The average mole fractions of deuterium in the two regions of $l_0 < z < l$ and $0 < z < l_0$ at τ are noted by $y_{1,m}$ and $y_{2,m}$, respectively. These values are expressed in terms of $\rho_z(z,\tau)$ as follows:

$$y_{1,m} = \frac{\int_{l_0}^{l} \rho_z(z,\tau)\, y\, dz}{\int_{l_0}^{l} \rho_z(z,\tau)\, dz} \quad (2)$$

$$y_{2,m} = \frac{\int_{0}^{l_0} \rho_z(z,\tau)\, y\, dz}{\int_{0}^{l_0} \rho_z(z,\tau)\, dz}. \quad (3)$$

After substituting Eqs. 2 and 3 for the two integrations in Eq. 1 and modifying it using the following two relations

$$W = \int_0^{l} \rho_z(z,\tau)\, dz \quad (4)$$

and

$$W_0 = \int_0^{l_0} \rho_z(z,\tau_0)\, dz, \quad (5)$$

one gets the following equation:

$$\frac{y_{2,m}}{x_0} = \frac{y_{1,m}}{x_0} - \left(\frac{y_{1,m}}{x_0} + \frac{W_0}{W} - 1\right) \frac{\int_0^{l} \rho_z(z,\tau)\, dz}{\int_0^{l_0} \rho_z(z,\tau)\, dz}. \quad (6)$$

Equation 6 gives a unique relation between the deuterium concentration ratios of $y_{2,m}/x_0$ and $y_{1,m}/x_0$ and the ratio of the frost local density profile integrated from 0 to l to that from 0 to l_0. When a hypothetical frost density profile in the Appendix (Eq. A1), is substituted for $\rho_z(z,\tau)$ in Eq. 6, the following equation is obtained:

$$\frac{y_{2,m}}{x_0} = \frac{y_{1,m}}{x_0} - \left(\frac{y_{1,m}}{x_0} + \frac{W_0}{W} - 1\right) \frac{\dfrac{l}{l_0}}{1 + \delta\left(1 - \dfrac{l_0}{l}\right)}. \quad (7)$$

Thus, $y_{2,m}/x_0$ is a function of $y_{1,m}/x_0$, W_0/W, l/l_0, and δ.

On the other hand, a differential material balance equation in frost between the internal mass flux, $j_z(z,t)$, and the local frost density profile, $\rho_z(z,t)$, is derived from the assumption of the local mass flux in the horizontal direction being uniform:

$$\left(\frac{\partial j_z}{\partial z}\right)_t = \left(\frac{\partial \rho_z}{\partial t}\right)_z. \quad (8)$$

Integrating Eq. 8 from τ_0 to τ on t and from 0 to l_0 on z leads to the following equation:

$$\int_{\tau_0}^{\tau} j_z(l_0, t)\, dt = \int_0^{l_0} \rho_z(z, \tau)\, dz - \int_0^{l_0} \rho_z(z, \tau_0)\, dz. \quad (9)$$

Substitution of Eqs. 4, 5, and 6 for integrations in the right-hand side of Eq. 9 leads to the equation:

$$\frac{1}{W - W_0} \int_{\tau_0}^{\tau} j_z(l_0, t)\, dt = \frac{y_{1,m} - x_0}{y_{1,m} - y_{2,m}} + \frac{y_{2,m} W_0}{(y_{1,m} - y_{2,m})(W - W_0)}. \quad (10)$$

The lefthand side of Eq. 10 means the ratio of the internal mass flux at l_0 integrated from τ_0 to τ to the mass deposited per unit frost surface area. The term is expressed using the hypothetical internal mass flux profile in the Appendix (Eq. A5), as follows:

$$\frac{1}{W - W_0} \int_{\tau_0}^{\tau} j_z(l_0, t)\, dt = \frac{(1+\delta)\left\{\left(\frac{W}{W_0}\right)^{\beta} - 1\right\} - \delta\left\{\left(\frac{W}{W_0}\right)^{2\beta - 1} - 1\right\}}{W}. \quad (11)$$

Thus, the experimental values of $y_{2,m}/x_0$, $y_{1,m}/x_0$, W/W_0, and l_0 give information on the integration of $j_z(z, t)$, as seen in Eq. 11. The net mass flux on frost surfaces, j_t, was almost constant regardless of frosting time under properly selected experimental conditions (Fukada et al., 1995a,b; White and Cremers, 1981). Then we can replace W/W_0 in Eqs. 6, 7, 10, and 11 by τ/τ_0 under the constant j_t condition. With the replacement of W/W_0 by τ/τ_0, one gets information on the local density profile or the internal mass flux without knowing the j_t or W/W_0 value.

Experimental Studies

The experimental apparatus used in the present study is the same as was used in our previous study (Fukada et al., 1995a,b). The apparatus comprises an upper horizontal cooled plate and a lower warmed plate which are maintained respectively at constant temperatures. A side wall is made of glass for heat insulation. Vapor is evaporated from a pool of water on the lower plate, and frost is formed on the upper plate. Atmospheric gas is air. The Ra number defined using the plate width is in the range of 5×10^4 to 5×10^6, and the natural convection is generated between the two horizontal plates. The values of W and l were uniform in the horizontal direction over the cooled surface.

The experimental procedures were as follows. Frost was formed using the natural abundance of distilled water from 0 to τ_0. The values of W_0 and l_0 were determined at τ_0. The time τ_0 was 30 min or 1 h. The l_0 value was from 3.0 mm to 5.4 mm, depending on T_{w1} and p_t. At τ_0, the water was replaced by heavy water with a deuterium mole fraction of 5.0%. After the total frosting time τ elapsed, frost was cut out with a razor at a height of l_0 at several points of the upper plate. The time τ was set in the range of 1 h to 5.5 h. The l value was from 4.4 mm to 12.2 mm. The lower and upper parts of the frost were divided, and the average deuterium concentrations of the lower part ($0 < z < l_0$) and the upper part ($l_0 < z < l$) were measured by means of a quadrupole mass spectrometer. The frost amount necessary for the measurement of the deuterium concentration was 50 μL at the outside. The deuterium concentration was determined by a similar method in Thomas (1950).

The experimental conditions of the frost formation were in the range of 216 K $< T_{w1} <$ 253 K for the cooled wall temperature, $T_{S2} = 306$ K for the warmed water surface temperature, and $p_t = 1.0\times10^5$ Pa and 2.0×10^4 Pa for the total pressure in the container.

There are isotopic differences in the freezing point among H_2O, HDO, and D_2O. In the present experiment, almost all deuterium in water was present in the HDO form because of the low deuterium concentration. The ratio of the saturation vapor pressure of H_2O to that of HDO ($= P_{H_2O}/P_{HDO}$) was estimated 1.12 at 0°C. The isotopic difference makes H_2O evaporate from the water pool preferentially. Therefore, there is a possibility that the deposition deuterium concentration, x_0, varies with the passing of time and, consequently, is different from $y_{1,m}$. This is because of back diffusion from the lower part of $0 < z < l_0$ or a change in the deuterium concentration in the pool. The x_0 value was determined by using the same 5% heavy water from 0 to τ. The frost deuterium concentrations were found to be almost the same. The $y_{1,m}/x_0$ value was 1.0 ± 0.06 regardless of τ, T_{w1}, and p_t. Thus, x_0 was considered consistent with $y_{1,m}$ within experimental errors.

Results

Figure 2 shows variations of the deuterium mole fraction ratio, $y_{2,m}/x_0$, with the W/W_0 ratio. Curves in the figure are calculated using Eq. 7 based on the hypothetical local density profile of Eq. A1 in the Appendix, on the assumption that the $y_{1,m}/x_0$ value is unity from the preliminary experiment and the relation of $l/l_0 = (W/W_0)^{0.5}$ from our previous research (Fukada et al., 1995a,b).

The following three things are noticed from a comparison of the experiment with the calculation. First the experimentally obtained $y_{2,m}/x_0$ values are almost consistent with the curve of $\delta = 0$, which means a flat profile of the local frost density in the perpendicular direction. The best fitting value was $\delta = 0$ or $\delta = -0.1$, as shown below. The next thing is that there is a small deviation in variations of $y_{2,m}/x_0$ with W/W_0 under different T_{w1} and p_t conditions. The third thing is that $y_{2,m}/x_0$ becomes comparatively large when partial melting of the frost was observed on its surface or inside. When frost partly melts, a certain amount of water permeates its inside.

Figure 3 shows variations of the internal mass flux ratio, $\int_{\tau_0}^{\tau} j_z(l_0, t)\, dt/(W - W_0)$, with the mass ratio, W/W_0. Similar to Figure 2, the assumption of $y_{1,m}/x_0 = 1$ is set for the calculation. In order to make it clear whether or not the reduced values on the vertical axis are independent of T_{w1} and p_t, we

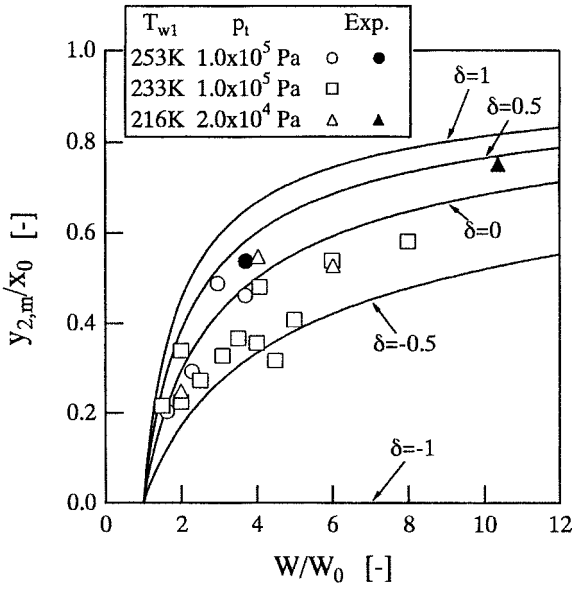

Figure 2. Variations of mole fraction ratio $y_{2,m}/x_0$ with mass deposition ratio W/W_0 (frost melting was observed under the conditions of the filled circle and triangle: ● and ▲).

determined the best fit value of δ in such a way that the standard deviation between Eq. 11 and the experimental data is minimized. The best fit value is $\delta = 0$ under the condition of $T_{w1} = 253$ K and $p_t = 1.0 \times 10^5$ Pa, $\delta = -0.1$ under $T_{w1} = 233$ K and $p_t = 1.0 \times 10^5$ Pa, and $\delta = -0.1$ under $T_{w1} = 216$ K and $p_t = 2.0 \times 10^4$ Pa. Thus, the experimental data support the idea that the internal mass flux decreases almost linearly, which corresponds to the curve of $\delta = 0$. The results are almost independent of T_{w1} and p_t.

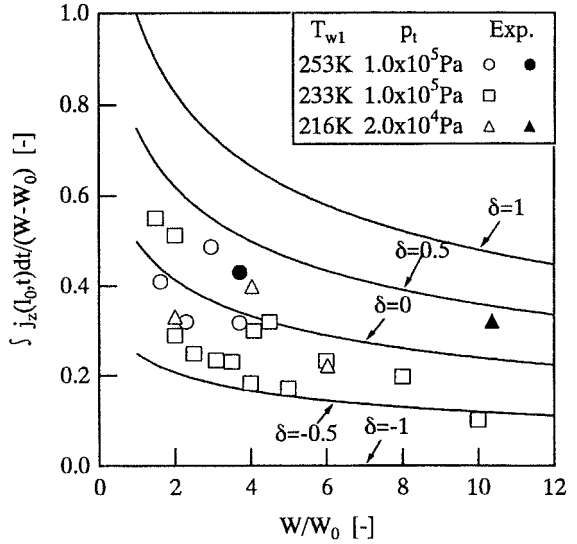

Figure 3. Variations of mass flux ratio $\int_{\tau_0}^{\tau} j_z(l_0,t)\,dt/(W - W_0)$ with mass deposition ratio W/W_0 (frost melting was observed under the conditions of the filled circle and triangle: ● and ▲).

When one extrapolates the data in Figure 3 to $W/W_0 = 1$, the ratio of the internal mass flux to the total mass flux on frost surfaces, $j_z(l,\tau)/j_t(=\beta)$, may become 0.5. The relation of $\beta = 0.5$ is consistent with the righthand side of Eq. A5 in the Appendix. This result supports the parabolic growth rate rule of frost that was empirically assumed in previous analyses by Schneider (1978), White and Cremers (1981), Saito et al. (1984), and Ostin and Anderson (1991). Our experimental work on the internal mass flux proved the empirical parabolic growth rate rule for the first time.

Discussion

Internal mass flux and internal temperature distribution

The internal mass-flux profile in the z-direction has been evaluated using the internal diffusion vapor flux, $j_{\text{diff}}(z,t)$, as a function of the saturation vapor pressure, p_{sat} (Woodside, 1958; Brian et al., 1970; Biguria and Wenzel, 1970; Yamakawa et al., 1972; Jones and Parker, 1975; Hayashi et al., 1977b):

$$j_{\text{diff}}(z,t) = \frac{D_{AB}\,p_t}{\tau_s R_g T(p_t - p_{\text{sat}})}\frac{dp_{\text{sat}}(T)}{dz}. \qquad (12)$$

The diffusion coefficient D_{AB} in Eq. 12 decreases inversely with the increase in p_t. Therefore, $j_{\text{diff}}(z,t)$ should depend on p_t. However, this pressure dependence conflicts with the present experimental results on $j_z(z,t)$.

Judging from Figure 2, $\rho_z(z,t)$ is almost uniform in the perpendicular direction. Therefore, it is also expected that the local frost thermal conductivity, λ_z, is constant over the whole frost. With the constant λ_z, the heat balance equation inside the frost under a quasisteady state is described as follows (Jones and Parker, 1975):

$$\lambda_z\frac{d^2T}{dz^2} = -L_V\frac{dj_z}{dz}. \qquad (13)$$

Substituting $j_z = \beta j_t z/l$ for j_z in Eq. 13 and integrating it under the boundary conditions of $T = T_{w1}$ at $z = 0$ and $\lambda_z dT/dz = q_t - \beta j_t L_v$ at $z = l$ lead to the following temperature profile inside the frost:

$$T = T_{w1} + \frac{q_t z}{\lambda_z} - \frac{\beta j_t L_V z^2}{2\lambda_z l}. \qquad (14)$$

Figure 4 shows an example of the variations of the frost temperature measured at several specified positions with time. The temperature variations calculated from Eq. 14 agree comparatively well with the experimental ones. However, vapor-pressure profiles calculated from the temperature profile did not make up the linear internal mass flux. The inconsistency might be improved by assuming a certain supersaturation condition, that is, by replacing $p_{\text{sat}}(T)$ in Eq. 12 by $p_{\text{crit}}(T)$. If the system were below the critical supersaturation condition, the variations of the vapor flux along the direction of the frost depth could be linear, independent of temperature profile. The supersaturation ratio, $S(=p_{\text{crit}}/p_{\text{sat}})$, was

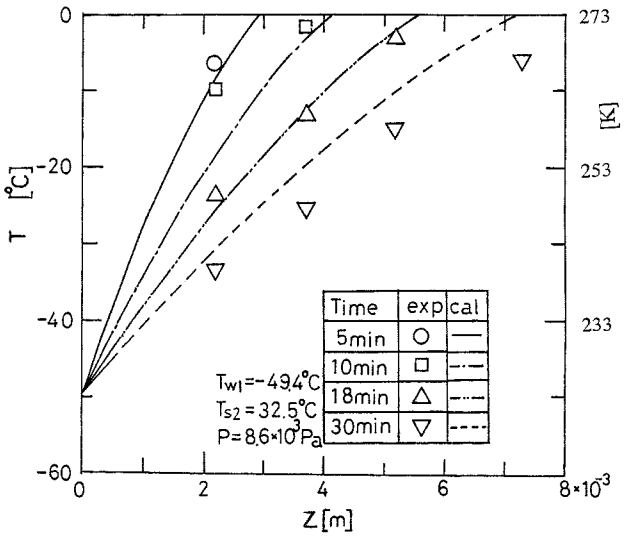

Figure 4. Variations of temperature in frost with time and space.

evaluated based on the critical supersaturation model (Epstein and Rosner, 1970). However, it was found that the two conditions in Figures 2 and 3 ($T_{w1} = 233$ K and 216 K) were by far over the critical supersaturation condition. Consequently, the inconsistency was hardly improved, even by assuming the critical supersaturation in the system.

The inconsistency on the internal mass flux between Eq. 12 and experimental ones was also reported by Brian et al. (1970) and Dietenberger (1983), who determined the local frost density directly. Brian et al. (1970) proposed two overall balance equations on heat and mass transfer and another material balance equation on vapor flux on the frost surface that gives the internal frost growth rate quantitatively. The former two conservation equations succeeded in evaluating the total mass deposition rate, the total heat flux, and the increased rate of the average frost density. However, the third equation using Eq. 12 failed to fit the increased rate of the local frost density. Thus, the vapor diffusion model based on Eq. 12 did not agree with the previous experimental results.

Cause of the linear internal mass flux

Here, we discuss the causes of the linearity of the internal mass flux or the uniformity of the local frost density. The uniformity should be held regardless of T_{w1} and p_t. An explanation for them also should be consistent with previous experimental results on frost properties.

First of all, there is one point that always has been ignored in the third material balance equation. It is the effect of crystal growth on frost formation. The local material balance equation inside the frost may be described in terms of the crystal growth rate as follows:

$$\frac{\partial \rho_z}{\partial t} + \boldsymbol{\nu} \cdot \nabla \rho_z = \left(1 - \frac{\rho_z}{\rho_{\text{ice}}}\right) \nabla \cdot j_{\text{diff}}. \tag{15}$$

The first term on the lefthand side of Eq. 15 expresses the intrinsic increased rate of the local frost density. The second term is the contributions of the internal frost growth, both in the longitudinal direction and in the horizontal direction. When the crystal growth rate is sufficiently fast in any direction, that is, when $\boldsymbol{\nu}$ is large, the relation of $\nabla \rho_z \fallingdotseq 0$ can be reasonably reduced from Eq. 15. Thus, the isotropic frost properties are related to the microscopic crystal growth rate through Eq. 15. Earlier researchers regarded dendrite frost as a stationary phase. However, one needs to see it as a mobile phase. This change of view may include the idea that $\nabla \cdot j$ in Eq. 8 is actually related not to $\nabla \cdot j_{\text{diff}}$ but to $(1 - \rho_z/\rho_{\text{ice}})\nabla \cdot j_{\text{diff}} - \boldsymbol{\nu} \cdot \nabla \rho_z$. Simply put, the second term is related with frost migration due to the microscopic growth. Therefore, $\nabla \cdot j_{\text{diff}}$ does not need to agree with $\partial \rho / \partial t$. Thus, the idea of j_{diff} defined by Eq. 12 being inconsistent with j_z becomes somewhat understandable.

Generally speaking, the frost growth rate should be described quantitatively based on a microscopic crystal-growth equation. However, the equation is very difficult to solve strictly, so we deal with it in a simplified way. If frost crystals grow on nucleation points, the relation between the crystal growth rate on each nucleation point, v_i, and the internal diffusion flux can be approximated by the equation:

$$\nabla \cdot j = \sum_{i=1}^{N} \nu_i \rho_i. \tag{16}$$

The summation in Eq. 16 is made over all nucleation points, N. When frost is isotropic, v_i is independent of the growth direction. If the product of v_i and ρ_i is assumed to be the same on every nucleation point, Eq. 16 will be simplified to the following equation in terms of the angle of each growth direction with the z-direction defined as θ_i:

$$\nabla \cdot j = (\nu_i \rho_i)_{\text{cry}} \sum_{i=1}^{N} \theta_i. \tag{17}$$

Furthermore, Eq. 17 can be rewritten to the equation under the condition of homogeneous frost:

$$\nabla \cdot j = (\nu_i \rho_i)_{\text{cry, up}} + (\nu_i \rho_i)_{\text{cry, down}}. \tag{18}$$

The first term on the righthand side of Eq. 18 is related to the upward growth rate corresponding to $\rho dl/dt$, which means the frost growth in the vertical direction. The second term is related to the downward crystal growth rate corresponding to $ld\rho/dt$, which means the growth in the horizontal direction. The ratio $(\rho dl/dt)/(ld\rho/dt)$ should be unity under isotropic frost. Consequently, the β value always becomes 0.5. Consequently, the assumption by White and Cremers (1981) can be understood well based on the isotropic and homogeneous properties of the frost without considering j_{diff}.

At the initial stage of the frost formation, the perpendicular frost growth prevails over other directions because of the large temperature gradient (Okubo and Tajima, 1983; Seki et al., 1984). When the crystal growth rate in the z-direction v_z is much higher than those in any other directions, terms except v_z on the lefthand side of Eq. 15 become negligible and

$\partial\rho_z/\partial z$ becomes comparatively small. Thus the frost thickness grows linearly in the z-direction. The number of the nucleation points increases during the induction period of frost formation. After the induction period, the one-dimensional frost growth ends. Then the three-dimensional or fractal frost growth becomes dominant, and the second term on the left-hand side of Eq. 15 becomes large in any direction. Consequently, a difference in the local frost density decreases. The local frost density is uniform unless frost melts. When frost melts partly, the internal mass flux becomes greater than those expected from its linear variation, as shown by the filled circles and triangles in Figures 2 and 3.

Conclusions

Experimental variations of the deuterium concentration in frost with time showed that the internal mass flux diffuses in such a way that frost grows uniformly in the perpendicular direction as well as in the horizontal direction, regardless of the cooled-plate temperature and the total pressure. The previous vapor diffusion model in frost failed to explain our experimental results as well as those of others. This was because the three-dimensional or fractal growth of isotropic frost was not included in the internal vapor-diffusion equation. If the growth rate on nucleation points is high enough, the uniformity of the local frost density is explained based on a simplified microscopic frost growth equation. This phenomenon was independent of the cooled temperature and the total pressure. It may depend on an intrinsic frost structure, such as whether or not frost is isotropic.

Notation

j = internal mass flux in frost, $\mathrm{kg\cdot m^{-2}\cdot s^{-1}}$
L_v = latent heat by sublimation, $\mathrm{J\cdot kg^{-1}}$
p_t = total pressure, Pa
q_t = total heat flux, $\mathrm{W\cdot m^{-2}\cdot K^{-1}}$
R_g = gas constant, $\mathrm{J\cdot kg^{-1}\cdot K^{-1}}$
T_{s2} = temperature on lower liquid surface, K
T_{w1} = temperature on upper cooled plate, K
t = time, s
v_{cry} = crystal growth rate, $\mathrm{m\cdot s^{-1}}$
z = distance from cooled surface, m
β = parameter for profile of internal mass flux appearing in Eq. A4
δ = parameter for profile of local frost density appearing in Eq. A1
ρ_{cry} = density of crystal, $\mathrm{kg\cdot m^{-3}}$
ρ_{ice} = density of ice, $\mathrm{kg\cdot m^{-3}}$
ρ_m = average frost density, $\mathrm{kg\cdot m^{-3}}$
τ = total time of frost formation, s
τ_s = tortuosity of frost

Literature Cited

Biguria, G., and L. A. Wenzel, "Measurement and Correlation of Water Frost Thermal Conductivity and Density," *Ind. Eng. Chem. Fundam.*, **9**, 129 (1970).

Brian, P. L. T., R. C. Reid, and Y. T. Stah, "Frost Deposition on Cold Surfaces," *Ind. Eng. Chem. Fundam.*, **9**, 375 (1970).

Dietenberger, M. A., "Generalized Correlation of the Water Frost Thermal Conductivity," *Int. J. Heat Mass Transfer*, **26**, 607 (1983).

Epstein, M., and D. E. Rosner, "Enhancement of Diffusion-Limited Vaporization Rates by Condensation within the Thermal Boundary Layer," *Int. J. Heat Mass Transfer*, **13**, 1393 (1970).

Fukada, S., S. Furuta, and N. Mitsuishi, "Mass Transfer with Mist Formation for Laminar Flow in Vertical Cooling Tube with Constant Temperature Wall—Experimental and Theoretical Study on Fuel Gas Refining System with Cryogenic Freezer," *J. Atom. Energy Soc. Jpn.*, **31**, 487 (1989a).

Fukada, S., K. Inoue, and N. Mitsuishi, "Effects of Presence of Foreign Nuclei on Mass Flux at Cooling Walls in Cryogenic Freezer," *J. Nucl. Sci. Technol.*, **26**, 808 (1989b).

Fukada, S., K. Inoue, and M. Nishikawa, "Frost Deposition on Cooled Surfaces under Reduced Pressure," *Kagaku Kogaku Ronbunshu*, **21**, 166 (1995a).

Fukada, S., H. Tsuru, and M. Nishikawa, "Frost Formation under Different Gaseous Atmospheres," *J. Chem. Eng. Jpn.*, **28**, 732 (1995b).

Fukada, S., Y. Fujii, and M. Nishikawa, "Mist Formation in a Water Vapor Cold Trap and Evaluation of Its Removal Rate," *J. Nucl. Sci. Technol.*, **35**, 198 (1998).

Hayashi, Y., S. Adachi, and K. Yamaguchi, "Frost Deposition by Natural Convection," *Cryogenics*, **52**, 707 (1977a).

Hayashi, Y., A. Aoki, S. Adachi, and K. Hori, "Study of Frost Properties Correlating with Frost Formation Types," *J. Heat Transfer*, **99**, 239 (1977b).

Jones, B. W., and J. D. Parker, "Frost Formation with Varying Environmental Parameters," *J. Heat Transfer*, **97**, 255 (1975).

Okubo, H., and O. Tajima, "The Frosting Phenomena to the Vertical Plate in Natural Convection Flow," *Refrigeration*, **58**, 3 (1983).

Ostin, R., and S. Anderson, "Frost Growth Parameters in a Forced Air Stream," *Int. J. Heat Mass Transfer*, **34**, 1009 (1991).

Saito, H., I. Tokura, K. Kishinami, and S. Uemura, "A Study on Frost Formation (on Dimensionless Parameters Correlating Density and Thickness of Frost Layer)," *Bull. JSME*, **50**, 1190 (1984).

Schneider, H. W., "Equation of the Growth Rate of Frost Forming on Cooled Surfaces," *Int. J. Heat Mass Transfer*, **21**, 1019 (1978).

Seki, N., S. Fukusako, K. Matsuo, and S. Uemura, "Incipient Phenomena of Frost Formation," *Bull. JSME*, **50**, 825 (1984).

Thomas, B. W., "Determination of Heavy Water by Mass Spectrometer," *Anal. Chem.*, **22**, 1476 (1950).

White, J. E., and C. J. Cremers, "Prediction of Growth Parameters of Frost Deposits in Forced Convection," *J. Heat Transfer*, **103**, 3 (1981).

Woodside, W., "Calculation of the Thermal Conductivity of Porous Media," *Can. J. Phys.*, **36**, 815 (1958).

Yamakawa, N., N. Takahashi, and S. Otani, "Heat and Mass Transfer by Forced Convection under the Frosting Condition," *Kagaku Kogaku*, **35**, 328 (1971).

Yamakawa, N., and S. Otani, "Heat and Mass Transfer in the Frost Layer," *Kagaku Kogaku*, **36**, 197 (1972).

Appendix: Hypothetical Local Density Profile

The present method using heavy water provides a strict way to determine the profiles of the internal mass flux in frost and the local frost density. At this stage of the present study, however, it was difficult to determine the whole profile of the internal mass flux exactly from the frost deuterium concentration. This is because both Eqs. 6 and 10 are written by an integration form that is integrated, respectively, from τ_0 to τ on t and from 0 to l on z. Therefore, we postulated hypothetical profiles of the local frost density and the internal mass flux. The deuterium concentration inside the frost, which was expected from the hypothetical profile, is compared with the experimental deuterium concentration. The hypothetical local density profile inside the frost is as follows:

$$\rho_z(z,\tau) = \rho_m\left\{1+\delta\left(1-\frac{2z}{l}\right)\right\}. \qquad \text{(A1)}$$

When $0<\delta<1$, the frost density in the smaller z region is higher than that in the larger z region. On the other hand, when $-1<\delta<0$, that in the larger z part is higher than that in the smaller z part. When $\delta=0$, it gives a flat density pro-

file. Thus δ is a parameter to characterize the local frost density profile. Equation 7 in the text is derived by substituting Eq. A1 for ρ_z in Eq. 6.

The substitution of Eq. A1 for ρ_z in Eq. 8 leads to the following equation of the internal mass flux:

$$\frac{\partial j_z}{\partial z} = (1+\delta)\frac{\partial}{\partial \tau}\left(\frac{W}{l}\right) - 2\delta z \frac{\partial}{\partial \tau}\left(\frac{W}{l^2}\right). \qquad \text{(A2)}$$

When the mass flux on frost surfaces is also constant, the following equation holds:

$$\frac{W}{\tau} = \frac{W_0}{\tau_0}. \qquad \text{(A3)}$$

Variations of the frost thickness with time were generally described by the following equation (White and Cremers, 1981):

$$\frac{l}{l_0} = \left(\frac{\tau}{\tau_0}\right)^{1-\beta}. \qquad \text{(A4)}$$

Inserting Eqs. A3 and A4 into Eq. A2 and integrating Eq. A2 from 0 to z leads to the equation

$$j_z(z,\tau) = j_t\left\{\delta(1-2\beta)\left(\frac{z}{l}\right)^2 + \beta(1+\delta)\frac{z}{l}\right\}. \qquad \text{(A5)}$$

When $\beta = 0.5$, the first term in the bracket on the righthand side of Eq. A5 disappears, and the frost thickness grows with the square root of time.

Manuscript received Apr. 5, 1999, and revision received Aug. 25, 1999.